Macromolecules

Article

pubs.acs.org/Macromolecules

Synthesis and Properties of an Electropolymer Obtained from a Dimeric Donor/Acceptor System with a 4,4′-Spirobi[cyclopenta[2,1-*b*:3,4-*b*′]dithiophene] Core

Simonetta Orlandi, Gianluca Pozzi,* and Marco Cavazzini

Istituto di Scienze e Tecnologie Molecolari del Consiglio Nazionale delle Ricerche, ISTM-CNR, via Golgi 19, 20133 Milano, Italy

Daniela Minudri, Miguel Gervaldo, Luis Otero, and Fernando Fungo*

Departamento de Química, Universidad Nacional de Río Cuarto, Agencia Postal 3 (X5804BYA), 5800 Río Cuarto, Argentina

ABSTRACT: The design and synthesis of two potentially electropolymerizable electron donor−acceptor dyes characterized by a cruciform 4,4′-spirobi[cyclopenta[2,1-*b*:3,4-*b*′]-dithiophene] core is here outlined. The new molecules feature two perpendicularly aligned cyclopentadithiophene branches, each one having an electrodimerizable, electron donor triphenylamine unit and an electron acceptor dicyanovinylene group. By merging these structural elements, the light absorption ability of the conjugated cyclopentadithiophene chromophore is extended to a broad region of the visible spectrum. The photoelectroactive film obtained from one of the dyes by electrochemical deposition technique retains the ability to generate photoinduced charge-separated states and to transport holes, turning this material into a unique example of donor−acceptor polymer with potential application in the development of organic optoelectronic devices.

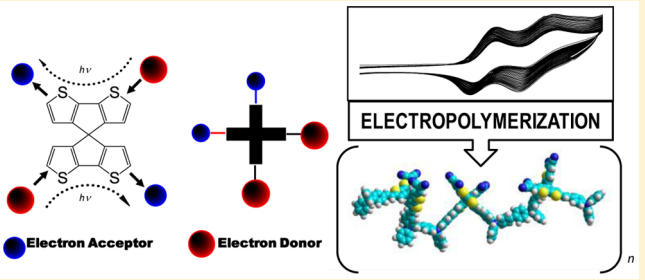

INTRODUCTION

The design and development of new polymeric functional material for application in organic optoelectronic devices, like polymer solar cells, is one of the most active areas of research, mainly due to the continuous search for low-cost renewable energy sources.[1] Flexibility, solution processability, and short energy payback time are among the very important characteristics of the organic-based materials that make possible their application in large area devices. Furthermore, structural modifications that allow tunable band gap permit the generation of tandem or multicolored solar cells. However, despite the facts that high power conversion efficiencies have been attained with bulk heterojunction structures,[2] and that the potentiality of the organic photovoltaic technology is still huge, to date industrial production and large scale commercialization have not been achieved,[3] a major issue being the transfer of the efficiencies obtained on small area cells to large area modules.[4] Thus, the development of new polymeric materials and devices construction methods are still necessary in order to find procedures that allow the implementation of this relevant technology.

One of the principal difficulties that the use of organic polymers in electronics has to face is the film deposition methodology over the conducting or semiconducting contacts.[5−8] The most common approaches rely on thermal evaporation and solution-processing methods. However, thermal evaporation requires materials with adequate sublimation capability and thermal stability, properties that are difficult to reach in polymers. Also, solution processes, such as dip- or spin-coating methodologies, require polymeric materials with intrinsic high solubility. On the contrary, electropolymerization of suitable photoelectroactive monomers allows the synthesis and formation of polymeric films in one step, with the possibility to get control over pattern and thickness, two very important aspects in the implantation of industrial processes. There are numerous antecedents showing that the polymeric films obtained electrochemically over conductive solid substrates are very stable, with excellent stuck and electrical contact with the base material.[9,10,17]

In the field of all-polymer solar cells, the synthesis of polymeric structures featuring a combination of both donor (D) and acceptor (A) blocks present in conjugated chains is currently the focus of intense interest.[18] Indeed, the use of a suitable D−A copolymer as the active component in an all-polymer solar cell can increase the power conversion efficiency (PCE) of the device by avoiding some of the adverse characteristics typical of polymer blends, such as phase segregation[19] and low crystallinity,[20] that limit the photoinduced generation and mobility of charge carriers. Regardless of this potential, only limited examples of photoactive D−A

Received: April 21, 2015
Revised: June 9, 2015

DOI: 10.1021/acs.macromol.5b00845
Macromolecules XXXX, XXX, XXX−XXX

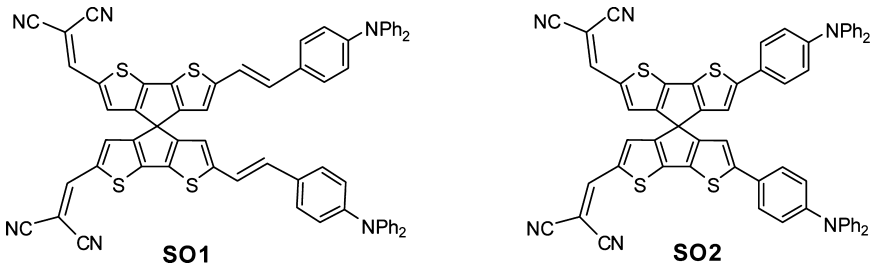

Figure 1. Dimeric donor/acceptor molecules investigated in the present work.

copolymers where both moieties are linked through conjugated bonds have been reported, mainly due to synthetic difficulties.[18] In this sense, the electrochemical synthesis methodology is also a powerful and little explored tool for the formation of polymers holding D and A moieties. In the past years we developed polymeric materials, produced by electrochemical methods, where both donor and acceptor groups, linked by a conjugated backbone, were already present in the structural monomer.[9−14,21,22] These materials exhibited photovoltaic and electrochromic properties[9−14,21] and were applicable in the construction of an electroluminescent device.[22] In all cases, monomers holding the spiro configuration were selected. In the spiro arrangement two identical or different π-conjugated systems are linked by a common sp^3-hybridized atom, leaving two perpendicularly oriented molecular halves. Spiro compounds are actively investigated as organic molecular materials for optoelectronics[23−25] due to their particular and favorable properties, such as morphological stability in solid state, reduced tendency to form aggregates, and improved solubility with respect to the corresponding nonspiro parent compounds. Furthermore, in this orthogonal arrangement the electronic interactions between the two halves are significantly reduced, and habitually the two π-systems can be perceived as independent compounds.[26,27] Several molecular systems based on spiro-configured units have found uses in electrochemiluminescence studies,[28] lasers,[29] electrochromic materials,[21,30,31] organic light-emitting devices,[22] organic field-effect transistors,[32] and solid-state dye-sensitized solar cells (DSSC).[24,33−36]

It is worth noting that most of the spiro compounds applied in optoelectronics, including those used in the construction of solar cells, are based on the 9,9′-spirobifluorene core. This field of research could be fruitfully expanded by introducing alternative spiro cores with different optic and electronic characteristics, as we recently demonstrated with the design of a spiro-configured bis-D-A derivative holding a 4,4′-spirobi[cyclopenta[2,1-*b*:3,4-*b*′]dithiophene] (SCPDT) core that was successfully used as a light absorber in DSSC.[37] The inclusion of two spiro-configured dithiophene residues as conjugated chromophore between the donor (triphenyl amine) and acceptor (cyanoacrylic acid) moieties allowed extending the sensitization process to the red region of the visible spectrum, producing a concomitant increment in the photocurrent generation.[37]

On the basis of this background, we have now designed and synthesized the electropolymerizable D−A monomers **SO1** and **SO2** derived from SCPDT (Figure 1). Their molecular structure features two perpendicularly aligned moieties, each one bearing the well-known dimerizable triphenylamine (TPA) unit as the electron donor and the dicyanovinylene group as the electron acceptor residue.[9,38]

These molecules were planned with the aim to achieve their polymerization through dimerization of the electrochemically generated TPA radical cations, giving rise totetraphenylbenzidine (TPB) substructures with hole transport capability. The presence of two spiro-configured molecular halves would then allow the generation of electroactive polymers. These materials would hold the capacity for the generation of photoinduced charge separated states, with light absorption in a broad region of the visible spectrum thanks to the presence of the bridging dithiophene units in the SCPDT centers.

EXPERIMENTAL SECTION

Synthetic Procedures. *Materials.* All available chemicals and solvents were purchased from commercial sources and were used without any further purification. 4,4′-Spirobi[cyclopenta[2,1-*b*:3,4-*b*′]dithiophene]-2,2′-dicarbaldehyde (**1**),[37] [4-(diphenylamino)-benzyl]triphenylphosphonium bromide (**2**),[39] 2,2′-dibromo-6,6′-diformyl-4,4′-spirobi[cyclopenta[2,1-*b*:3,4-*b*′]dithiophene] (**5**),[37] and 2,2′-bis[4-(diphenylamino)phenyl]-6,6′-diformyl-4,4′-spirobi-[cyclopenta[2,1-*b*:3,4-*b*′]dithiophene] (**6**)[37] were prepared as described in the literature. Solvents were purified by standard methods and dried if necessary. Reactions were monitored by thin layer chromatography (TLC) that was conducted on plates precoated with silica gel Si 60-F254 (Merck, Germany). Column chromatography was conducted by using silica gel Si 60, 230−400 mesh, 0.040−0.063 mm (Merck, Darmstadt, Germany).

Instrumentation. ^{1}H and ^{13}C NMR spectra were recorded on a Bruker Avance 400 (400 and 100.6 MHz, respectively); chemical shifts are indicated in parts per million downfield from $SiMe_4$, using the residual proton ($CHCl_3$ = 7.26 ppm) and carbon ($CDCl_3$ = 77.0 ppm) solvent resonances as the internal reference. Coupling constant values *J* are given in Hz. FTIR spectra were recorded on an Agilent Cary 630 infrared spectrophotometer. The high-resolution mass spectra were obtained with an electrospray ion-trap mass spectrometer ICR-FTMS APEX II (Bruker Daltonics) by the Centro Interdipartimentale Grandi Apparecchiature (C.I.G.A.) of the University of Milano. Elemental analyses were carried out by the Departmental Service of Microanalysis (University of Milano).

*2,2′-Bis-[(E)-(4-diphenylaminostyryl)]-4,4′-spirobi[cyclopenta[2,1-b:3,4-b′]dithiophene] (**3**).* In a flame-dried two-necked round-bottom flask equipped with a magnetic stirrer, [4-(diphenylamino)benzyl]-triphenylphosphonium bromide (**2**) (306 mg, 0.46 mmol) was introduced under an inert atmosphere and suspended in dry THF (25 mL). The mixture was cooled to −78 °C, and BuLi (1.6 M, 300 μL, 0.48 mmol) was added dropwise under stirring. After 2 h at −78 °C, a solution of **1** (50 mg, 0.13 mmol) in dry THF (5 mL) was slowly added in 40 min. The mixture was stirred for an additional hour at −78 °C, then the cooling bath was removed, and the mixture was allowed to return to RT and treated with water (5 mL). The organic layer was separated and the aqueous phase was extracted twice with Et_2O. The combined organic phase was washed twice with brine and dried over $MgSO_4$. After removal of the solvent at reduced pressure, the residue was purified by flash chromatography (silica gel, CH_2Cl_2:hexane 3:7) affording **3** (80 mg, 72% yield) as a yellow solid. ^{1}H NMR($CDCl_3$, 400 MHz): δ 7.27−7.22 (m, 12H), 7.11−7.08 (m, 10H), 7.04−6.97 (m, 8H), 6.93 (d, *J* = 16.0 Hz, 2H), 6.79 (d, *J* =

DOI: 10.1021/acs.macromol.5b00845
Macromolecules XXXX, XXX, XXX−XXX

Scheme 1. Synthesis of SO1 and SO2

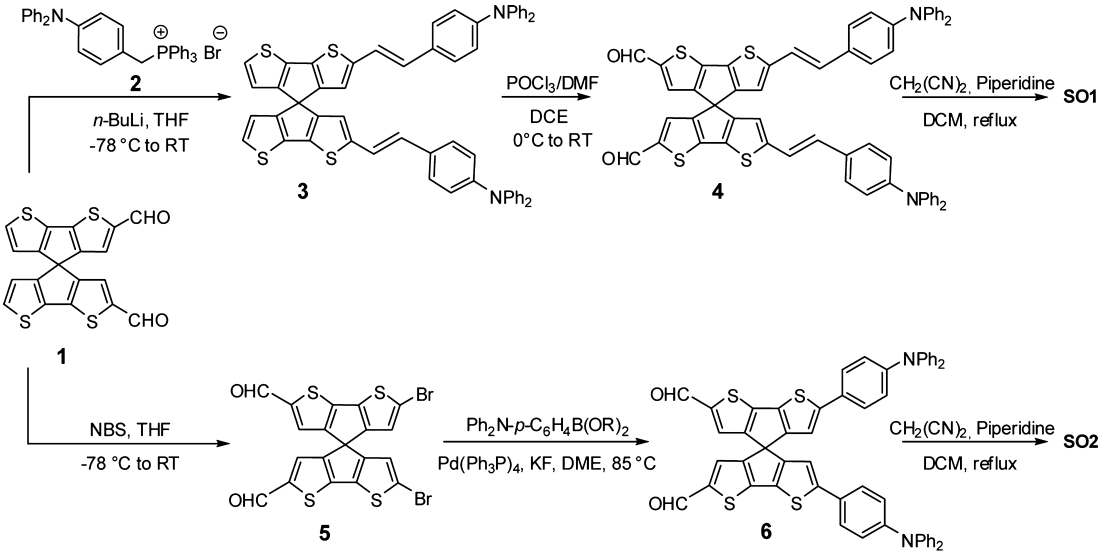

16.0 Hz, 2H), 6.54 (d, J = 4.9 Hz, 2H), 6.50 (s, 2H). ^{13}C NMR ($CDCl_3$, 100.6 MHz): δ 150.7, 150.2, 147.4, 147.2, 144.4, 138.9, 137.0, 131.0, 129.2, 127.0, 126.4, 125.8, 124.5, 123.4, 123.1, 121.4, 120.5, 119.6, 57.7. IR (KBr) ν (cm^{-1}): 1587, 1489, 1384, 1326, 1277, 1173, 1107, 831, 752, 695. HRMS (ESI): Calcd for $[C_{57}H_{38}N_2S_4]^+$: 878.19123. Found: 878.19295.

*2,2′-Diformyl-6,6′-bis-[(E)-(4-diphenylaminostyryl)]-4,4′-spirobi-[cyclopenta[2,1-b:3,4-b′]dithiophene] (**4**).* In a flame-dried two necked round-bottom flask equipped with a reflux condenser and a magnetic stirrer compound **3** (126 mg, 0.14 mmol) was dissolved under an inert atmosphere in dry 1,2-dichloroethane (DCE, 7 mL). The solution was cooled to 0 °C, and then dry DMF (40 μL, 0.52 mmol) followed by $POCl_3$ (60 μL, 0.64 mmol) was added. The mixture was stirred for 1 h at 0 °C, after which it was allowed to warm to RT, stirred for an additional hour, and finally refluxed for 2 h. After cooling, the reaction mixture was treated with aqueous AcONa (1M, 6 mL) and stirred for 1 h at RT. The organic phase was separated, and the aqueous phase was extracted twice with CH_2Cl_2. The collected organic phase was then washed with water and brine and dried over $MgSO_4$. After removal of the solvent at reduced pressure, the residue was purified by flash chromatography (silica gel, CH_2Cl_2:MeOH 100:0.5) affording the title compound **4** (102 mg, 76% yield) as a dark red solid. ^{1}H NMR ($CDCl_3$, 400 MHz): δ 9.69 (s, 2H), 7.27−7.23 (s, 12H), 7.21 (s, 2H), 7.1−7.08 (m, 8H), 7.06−7.02 (m, 4H), 7.00 (d, J = 8.8 Hz, 4H), 6.92 (m, 4H), 6.55 (s, 2H). ^{13}C NMR ($CDCl_3$, 100.6 MHz): δ 182.2, 154.0, 149.8, 149.5, 148.9, 148.0, 147.2, 144.1, 135.7, 129.8, 129.6, 129.3, 129.3, 127.4, 124.8, 123.4, 122.8, 119.4, 119.0, 57.5. IR (KBr) ν (cm^{-1}): 1651, 1586, 1490, 1384, 1314, 1262, 1218, 1137, 1102, 807, 752, 695. HRMS (ESI): Calcd for $[C_{59}H_{38}N_2O_2S_4Na]^+$: 957.17083. Found: 957.17259.

*2,2′-Bis(2,2-dicyanovinyl)-6,6′-bis-[(E)-(4-diphenylaminostyryl)]-4,4′-spirobi[cyclopenta[2,1-b:3,4-b′]dithiophene] (**SO1**).* In a two-necked round-bottom flask equipped with a reflux condenser and magnetic stirrer, compound **4** (70 mg, 0.074 mmol) was dissolved in dry CH_2Cl_2 (12 mL). After the addition of malononitrile (40 mg, 0.60 mmol) and piperidine (8 μL, 0.076 mmol) the solution was refluxed for 8 h. After cooling, the mixture was treated with water (7 mL), and the organic layer was separated. The aqueous phase was extracted twice with CH_2Cl_2, and the collected organic phase was washed thoroughly with water and dried over $MgSO_4$. After removal of the solvent at reduced pressure, the residue was purified by flash chromatography (silica gel, CH_2Cl_2:petroleum ether 8:2) affording **SO1** (54 mg, 71% yield) as a black solid. ^{1}H NMR($CDCl_3$, 400 MHz): δ 7.58 (s, 2H), 7.29−7.25 (m, 12H), 7.12−7.04 (m, 14H), 7.00−6.9 (m, 8H), 6.55 (s, 2H). ^{13}C NMR ($CDCl_3$, 100.6 MHz): δ 155.4, 152.63, 152.5, 149.7, 149.3, 148.4, 147.1, 136.2, 135.2, 130.7, 129.4, 129.3, 127.6, 125.0, 123.6, 122.5, 118.8, 118.7, 114.6, 114.1, 73.3, 56.8. IR (KBr) ν (cm^{-1}): 2217, 1587, 1561, 1508, 1487, 1384, 1293, 1173, 832, 753, 696. HRMS (ESI): Calcd for $[C_{65}H_{38}N_6S_4Na]^+$: 1053.19330. Found: 1053.20057. Anal. Calcd for $C_{65}H_{38}N_6S_4$: C 75.70, H 3.71, N 8.15. Found: C 75.68, H 3.72, N 8.11.

*2,2′-Bis(2,2-dicyanovinyl)-6,6′-bis(4-diphenylaminophenyl)-4,4′-spirobi[cyclopenta[2,1-b:3,4-b′]dithiophene] (**SO2**).* In a two-necked round-bottom flask equipped with a reflux condenser and magnetic stirrer, dialdehyde **6** (106 mg, 0.12 mmol) was suspended in $CHCl_3$ (16 mL). After the addition of a solution of malononitrile (90 mg, 1.36 mmol) in $CHCl_3$(10 mL) and piperidine (2.4 μL, 0.024 mmol), the mixture was refluxed overnight. After cooling, the mixture was treated with water (10 mL), and the organic layer was separated. The aqueous phase was extracted twice with $CHCl_3$, and the collected organic phase was washed thoroughly with water and dried over $MgSO_4$. After removal of the solvent at reduced pressure, the residue was purified by flash chromatography (silica gel, CH_2Cl_2:petroleum ether 9:1) affording **SO2** (60 mg, 50% yield) as a black solid. ^{1}H NMR ($CDCl_3$, 400 MHz): δ 7.58 (s, 2H), 7.36 (d, J = 8.7 Hz, 4H), 7.29−7.25 (m, 8H), 7.14 (s, 2H), 7.10−7.05 (m, 12H), 6.99 (d, J = 8.7 Hz, 4H), 6.72 (s, 2H). ^{13}C NMR ($CDCl_3$, 100.6 MHz): δ 155.96, 153.71, 152.90, 149.85, 149.14, 148.83, 146.91, 136.00, 135.21, 130.75, 129.49, 126.60, 126.46, 125.08, 123.89, 122.51, 116.04, 114.69, 114.17, 73.14, 57.15. IR (KBr) ν (cm^{-1}): 2215, 1561, 1482, 1384, 1303, 1169, 822, 752, 694.HRMS (ESI): Calcd for $[C_{61}H_{34}N_6S_4]^+$: 978.17223. Found: 978.17037. Anal. Calcd for $C_{61}H_{34}N_6S_4$: C 74.82, H 3.50, N 8.58. Found: C 74.86, H 3.50, N 8.55.

Photophysical, Electrochemical, and Photoelectrochemical Characterization. Electrochemical experiments were carried out in a homemade three-electrode Pyrex cell at room temperature with a potentiostat Autolab (Electrochemical Instruments). The electrolyte solution was a 0.1 M tetra-*n*-butylammonium perchlorate (TBAP) in anhydrous 1,2-dichloroethane solution. A glass inlaid platinum disk (2.16×10^{-3} cm^2) was used as working electrode. The Pt electrode was polished on a felt pad with 0.3 μm alumina, cleaned up by ultrasonication in water and absolute ethanol for 3 min, and then dried in an oven at 50 °C. A silver wire was used as a pseudoreference electrode, and a platinum coil was used as the counter electrode. After each electrochemical experiment, ferrocene was added to the electrolyte solution as internal standard, and the potential values reported in this study are expressed relative to the ferrocene/ferrocenium redox couple (Fc/Fc^+ = 0.40 V vs SCE).[40]

For spectroelectrochemical experiments the polymer was electrochemically grown on semitransparent ITO (indium tin oxide, Delta Technologies, 10 Ω/square) electrodes under the experimental conditions described above. Then, the ITO-coated glasses (pieces

DOI: 10.1021/acs.macromol.5b00845
Macromolecules XXXX, XXX, XXX−XXX

that fit in a standard UV−vis cuvette) under applied potential control were positioned in the optical pathway of a diode array spectrophotometer (Hewlett-Packard. Model 8453). A platinum wire was used as the counter electrode, and silver wire as the reference in a homemade cell.

For spectroelectrochemical experiments in monomer solution, a thin layer cell was used. Two ITO electrodes were sandwiched using a 60 μm spacer. The working electrode was placed with the conductive side facing inside the thin layer, and the counter electrode was placed facing the outside region of the thin layer. The pseudoreference electrode was a silver wire. The sandwiched cell was introduced in a commercial UV/vis cuvette containing 0.5 mL of **SO#** solution, where the thin layer was filled by capillarity.

RESULTS AND DISCUSSION

Synthesis of Monomers. The unusual stereoelectronic properties of SCPDT have been highlighted by computational studies,[41] but only a few molecules containing such a motif have been documented,[42,43] mostly because of their challenging synthesis. Only recently, a convenient access to the SCPDT core based on the Fe(III)-catalyzed intramolecular cyclization of a protected carbinol intermediate has been disclosed by us.[37] In that instance, it has been also found that the two halves of the highly symmetrical SCPDT molecule can be selectively functionalized taking advantage of the deactivating effect exerted by electron withdrawing substituents such as formyl groups. This effect can be exploited for the preparation of C_2-symmetric SCPDT derivatives where the 2- and 6-positions of each cyclopentadithiophene moiety hold one electron-donating and one electron-withdrawing substituent, respectively. We surmised that by introducing suitable substituents at those positions, the generation of D−A electropolymers from C_2-symmetric SCPDT monomers could be feasible. Our hypothesis has been tested starting with the TPA-functionalized molecules **SO1** and **SO2** that were conveniently obtained (Scheme 1) starting from the common precursor 2,2′-diformyl-4,4′-spirobi[cyclopenta[2,1-*b*:3,4-*b*′]dithiophene (**1**).[37]

The Wittig reaction between **1** and 4-(diphenylamino)-benzyltriphenylphosphonium bromide (**2**) allowed the introduction of two 4-diphenylaminostyryl moieties onto the SCPDT core. Compound **3** was obtained in good yield (72%) by slow addition of **1** to a solution of the phosphonium ylide generated by reaction of **2** with butyllithium as a base. This procedure avoided the massive formation of deformylation byproducts which is known to occur in Wittig−Horner reactions with thienyl carbaldehydes.[44] The subsequent selective formylation of **3** in the 6,6′-position of the SCPDT core was readily achieved under Vilsmeier reaction conditions, giving dicarbaldehyde **4** in good yield (76%). The targeted compound **SO1** was finally obtained in 71% yield by Knoevenagel condensation of **4** with malononitrile in the presence of piperidine. Similarly, the reaction between dicarbaldehyde **6**, obtained from **1** as previously reported,[37] and malononitrile in the presence of piperidine provided the monomer **SO2** in 51% yield.

Photophysical Properties. The steady-state absorption and emission spectra of the **SO#** molecules in aprotic solvents are shown in Figure 2.

For both dyes, four light absorption peaks can be distinguished in the absorption spectra, three of them having the maximum in the UV region, the remaining peak being a broad band with the higher extinction coefficient in the visible region. This optical behavior is in agreement with the reported ones for related molecular structures[10,37] The ultraviolet

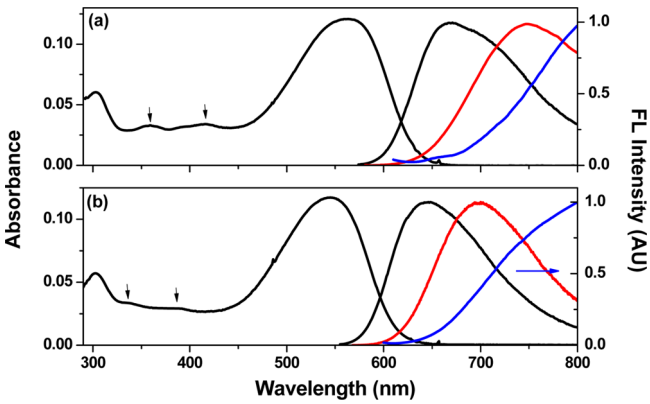

Figure 2. (a) Absorption (black line: toluene) and photoluminescence (black line: toluene, λ_{ex} = 563 nm; red: chloroform, λ_{ex} = 565 nm; blue: acetonitrile, λ_{ex} = 548 nm) spectra of **SO1**. (b) Absorption (black line: toluene) and photoluminescence (black line: toluene, λ_{ex} = 544 nm; red: chloroform, λ_{ex} = 555 nm; blue: acetonitrile, λ_{ex} = 532 nm) spectra of **SO2**. Absorption spectra in different solvents are nearly superimposed and are not shown for clarity.

absorption bands are associated with the $\pi-\pi^*$ electronic transition in bithiophene cores and TPA residues. On the other hand, the absorption in the visible region corresponds to donor−acceptor intramolecular charge transfer processes (ICT). Also, the high absorption intensity for the ICT bands indicates that the planarity of each bithiophene moiety, conferred by the **SO#** dyes molecular structure, maximizes the photostimulated charge transfer process.[37,45−47]

From a comparison of the specific absorption data for both dyes (Figure 2) it is observed that the light absorption maximum of **SO1** is red-shifted with respect to that of **SO2**. For example in toluene solution the ICT band maximum for **SO1** lies 19 nm at longer wavelength compared to **SO2**. This indicates that the introduction of a double bond between the bithiophene core and the TPA group in **SO1**, extending the π-conjugation lengths between the electron donor and acceptor moieties, produces a concomitant effect on the dye optical properties. On the other hand, Figure 2 also shows that the **SO#** dyes are fluorescent, when they are excited with light which energy corresponds to the ICT transition. The emission maximum of **SO1** is red-shifted with regard to **SO2**, in correlation with light absorption.

The **SO#** dyes absorption and emission spectra were evaluated in aprotic solvents with different polarities. For both dyes the absorption bands present slight hypsochromic shifts, which are observed when the change in solvent polarity is remarkable. For example, in the case of **SO1**, the ICT band maximum moves 15 nm toward the blue when the solvent is changed from toluene to acetonitrile (CH_3CN), while for **SO2** this displacement is of 14 nm. This behavior indicates that there is some degree of electronic coupling between the TPA electron donor and the dicyanovinylene electron acceptor moieties in the ground state. In contrast, **SO#** dyes emission maxima are strongly dependent on the solvent polarity. For **SO1** excited at ICT band wavelength in toluene solution the emission band maximum appears at 667 nm, and upon increasing the solvent polarity (chloroform), the emission band is red-shifted to 748 nm (Figure 2). Similar behavior is observed for **SO2**, for which the maximum emission band moves from 645 nm (toluene) to 698 nm (chloroform). Likewise, in CH_3CN the emission bands of both dyes move

DOI: 10.1021/acs.macromol.5b00845
Macromolecules XXXX, XXX, XXX−XXX

more than 150 nm toward the red, shifting their wavelength luminescence maximum out of the detector range of the used equipment (Figure 2).

These results are indicative of the formation of a polarized excited state associates to an intramolecular charge transfer process from the electron-donating to the electron-acceptor groups. This hypothesis is reinforced by the distribution of the frontier molecular orbitals (Figure 3) that shows the highest

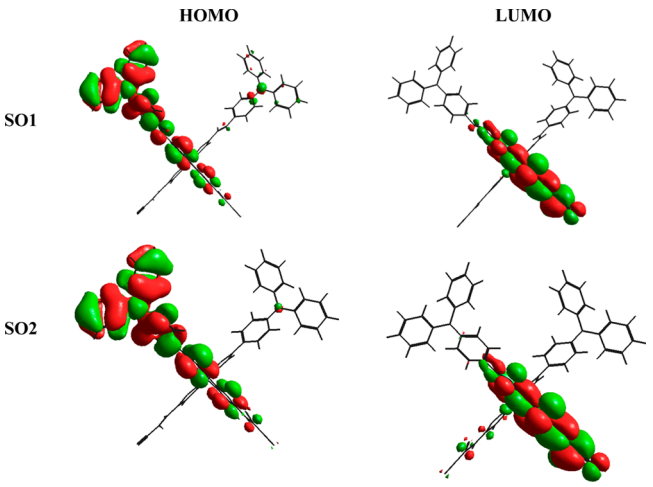

Figure 3. Geometric optimization (AM1 semiempirical calculations at HyperChem software) of **SO#** molecular structures. The HOMO and LUMO frontier molecular orbitals are shown.

occupied molecular orbital (HOMO) principally localized on the TPA groups and the lowest unoccupied molecular orbital (LUMO) on the dicyanovinylene residues.

In summary, **SO#** dyes present excellent light absorption capability over of a wide energy range, with the formation of highly directional charge separated states. This phenomenon confers to these molecular structures a high potential for optoelectronic applications.

Electrochemical Propertiesof the SO# Dyes. Cyclic voltammetry (CV) was used to assess the redox properties and the stability of the radical ions generated from **SO#** dyes. In the first anodic scan of **SO1** on Pt electrode two redox processes were observed, as it is shown in Figure 4a (black line). Upon the reverse negative potential scan, two cathodic peaks were detected, which are reduction complementary processes of the above-described anodic peaks. The corresponding formal potentials are ~0.37 V (processes I) and ~0.63 V (processes II) vs Fc/Fc^+. On the other hand, the CV waves proved that the stability of the oxidized products generated in both electrochemical processes is different. For the first couple the i_{pc}/i_{pa} (cathodic current peak/anodic current peak) ratio is close to one, while for the couple at 0.63 V the ratio is lower than one. This indicates that in the time scale of a CV scan the intermediates produced in the first oxidation processes are more stable than those formed in the second one. Moreover, repetitive scans between 0 and 0.55 V showed the same patterns as observed in the first scan (red line in Figure 4a). The first CV wave was only affected by the diffusion contribution, and the formation or growing of new peak systems was not detected under the present experimental conditions.

In contrast, when the potential scans were continuously cycled in a range that involves the second oxidation process, a

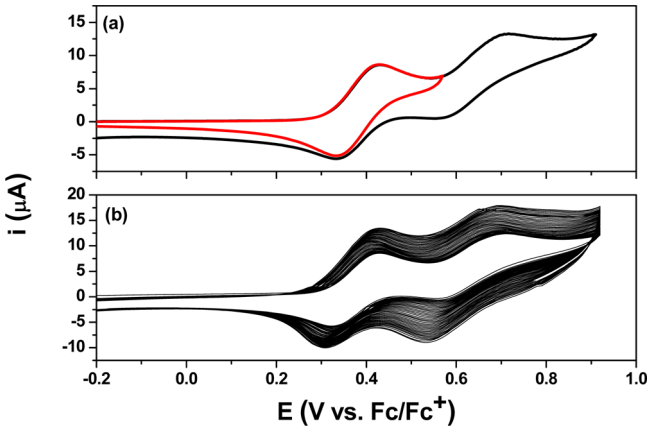

Figure 4. (a) Cyclic voltammograms of **SO1** (7.2×10^{-4} M) on Pt electrode in DCE with 0.1 M of TBAP, $V = 0.1$ V s^{-1}. (b) Repetitive cyclic voltammograms. $v = 0.1$ V s^{-1}; area of electrode = 3.14×10^{-2} cm^2.

progressive growth of current values in both peaks was observed (Figure 4b). This behavior can be associated with an oxidative coupling of **SO1** radical cations that produces an electroactive and conductive layer onto the electrode, as it is expected for molecules holding two or more independent TPA residues in their structure.[10,16,38]

In order to confirm this hypothesis, the modified Pt electrode obtained in the previous experiment was rinsed with fresh solvent to remove any **SO1** residue and immediately transferred to another cell with **SO1**-free electrolyte solution. Then, potential cycles between −0.2 and 1.0 V were applied to the electrode. The obtained current responses are reported in Figure 5.

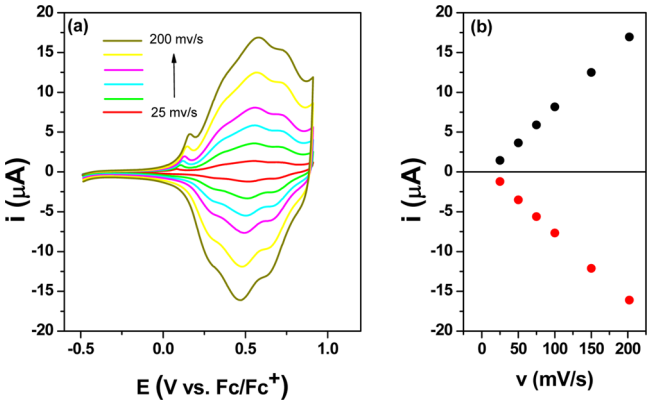

Figure 5. (a) Cyclic voltammograms of the electrodeposited film derived from **SO1** on a Pt electrode in DCE with 0.1 M of TBAP at different scan rates. (b) Plot of the experimental anodic and cathodic current peak as a function of scan rate (v). Area of electrode = 3.14×10^{-2} cm^2.

The cyclic voltammograms show wide oxidation waves, with a maximum at ~0.65 V (Figure 5a) and peak currents proportional to the potential scan rate (Figure 5b). In addition, the cycling between the neutral and oxidized states of the film for several minutes showed no degradation and/or current losses. All these observations are evidence of the formation of an irreversibly adsorbed electroactive product on the electrode surface.[10−16]

DOI: 10.1021/acs.macromol.5b00845
Macromolecules XXXX, XXX, XXX−XXX

On the other hand, the electrochemical response of the analogue **SO2** dye was found to differ from the behavior observed for **SO1**. The cyclic voltammogram (Figure 6) is still

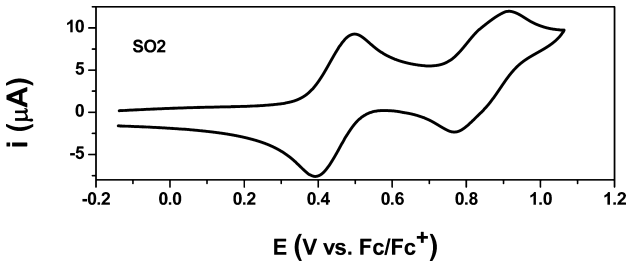

Figure 6. Cyclic voltammogram of **SO2** (6.8×10^{-4} M) on Pt electrode in DCE with 0.1 M of TBAP. $V = 0.1$ V s^{-1}; area of electrode = 3.14×10^{-2} cm^2.

characterized by two active redox couples at ~0.44 and ~0.83 V, but at difference of **SO1**, the stability of the oxidized products generated in both electrochemical processes quite similar, with i_{pc}/i_{pa} ratio close to one for both processes, indicating that all intermediates produced are stable in the time scale of a CV scan.

Moreover, for **SO2**, repetitive scans at inversion applied potential beyond the second oxidation process produce the same pattern as that observed in the first scan, without any current growing. The CV waves are only affected by the mass diffusion process to the electrode, and the formation of new redox systems was not detected under the present experimental conditions. This behavior indicates that the electrooxidized **SO2** species are more stable than those produced by the oxidation of **SO1**, and they cannot give rise to electrodeposited films on the Pt electrode surface.

The spiro compounds **SO1** and **SO2** are very similar at a molecular level since they are both composed of two identical D/A cyclopentadithiophene halves connected by a sp^3 carbon (Figure 1). **SO1** only differs from **SO2** for the presence of an additional C−C double bond between the TPA moiety and the cyclopentadithiophene unit. As already mentioned, the spiro conformation efficiently impedes the electronic interaction between the two identical molecular halves which can be thus roughly considered as independent entities whose redox and optical properties are not affected by their proximity. Therefore, the electrochemical response of the whole molecule can be inferred from the analysis of one of its halves.[10,12,23,24,28] In this way, two oxidizable centers can be identified in **SO#** dyes, namely cyclopentadithiophene and TPA. Based on previous electrochemical studies of related molecular structures,[10,12,16,37,48] it is plausible to propose that the oxidation potential of cyclopentadithiophene is lower than that of the TPA terminal moiety. One can thus assign the first electrochemical process in **SO#** molecules to the oxidation of cyclopentadithiophene π-system and the second one to the generation of TPA radical cation.[10,16] In the case of **SO1**, the formation of TPB groups through dimerization of TPA radical cation allows the surface electrode modification with an electroactive polymeric film[12,16] (see spectroelectrochemical study below). It can be also observed that for **SO1** both the oxidation of cyclopentadithiophene (0.37 V) and that of TPA (0.63 V) occur at lower anodic applied potential than the analogous processes for **SO2** (0.44 and 0.83 V, respectively). In agreement with this behavior, the ICT electronic transition in **SO1** occurs at lower energy values than the observed for **SO2** as outlined in the preceding section. Both electrochemical and spectroscopic data thus indicate that the introduction of one extra C−C double bond between the TPA moiety and the cyclopentadithiophene unit effectively increase the conjugation length in **SO#** dyes with significant consequences on the radical cations delocalization, as previously observed for related molecular systems.[10,11]

Spectroelectrochemical Characterization of the Electrogenerated Film. In order to study the optical characteristics of the electropolymer generated from **SO1** and to identify the species involved in the electrochemical processes in the organic film, a **SO1** polymeric thin film was formed over a semitransparent conductive electrode (ITO). This polymer-modified electrode will now be referred to as **ME-SO1**.

The spectroelectrochemical behavior of **ME-SO1** at different applied potentials, plotted as Abs and ΔAbs vs wavelength, is summarized in Figures 7a and 7b, respectively. When the film is

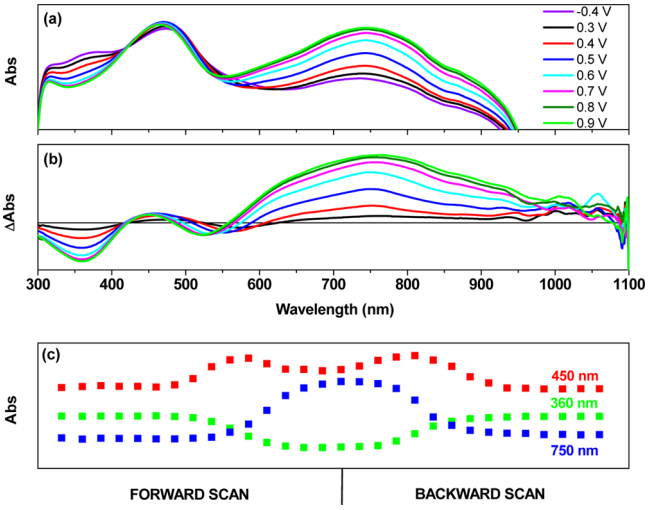

Figure 7. (a) Absorption spectra of the electrodeposited film of molecule **SO1** on an ITO electrode at various applied potentials in DCE with 0.1 M of TBAP. (b) Spectra plotted ΔAbs. (c) Absorption traces at selected wavelengths as a function of theadvances in the forward and backward CV scans.

in reduced state (−0.4 V), an intense absorption band with λ_{max} = ~475 nm is evident, showing that the ICT transition is retained in the polymer. However, there is a blue-shift of this transition (~75 nm) with respect to that observed for the monomer in solution. The participation of TPB units (formed by TPA dimerization in the polymer formation) as electron donor in the film should move the ICT to the red, due to the fact that TPB is oxidized with lower energy than TPA.[10,17,22,49] Thus, the blue-shift observed for the ITC transition in the film can be reasonably ascribed to the changes in the surrounding environment, originated in the solid state embedded in an electrolyte solution.[10,11,17,22] At the onset of the oxidation process the film presents a small increment of absorbance in the wavelength zone of 425−475 nm and a bleaching of the band at higher energy ($\lambda_{max} \approx 360$ nm). This effect can be fully appreciated in Figure 7b. When the applied potential becomes more anodic, a broad band centered at 750 nm grows, which reaches its maximum value at the end of the oxidation process (0.9 V). Figure 7c shows the traces at the main absorption values during an oxidation/reduction cycle. It can be clearly

DOI: 10.1021/acs.macromol.5b00845
Macromolecules XXXX, XXX, XXX−XXX

Scheme 2. Polymerization Mode of SO1

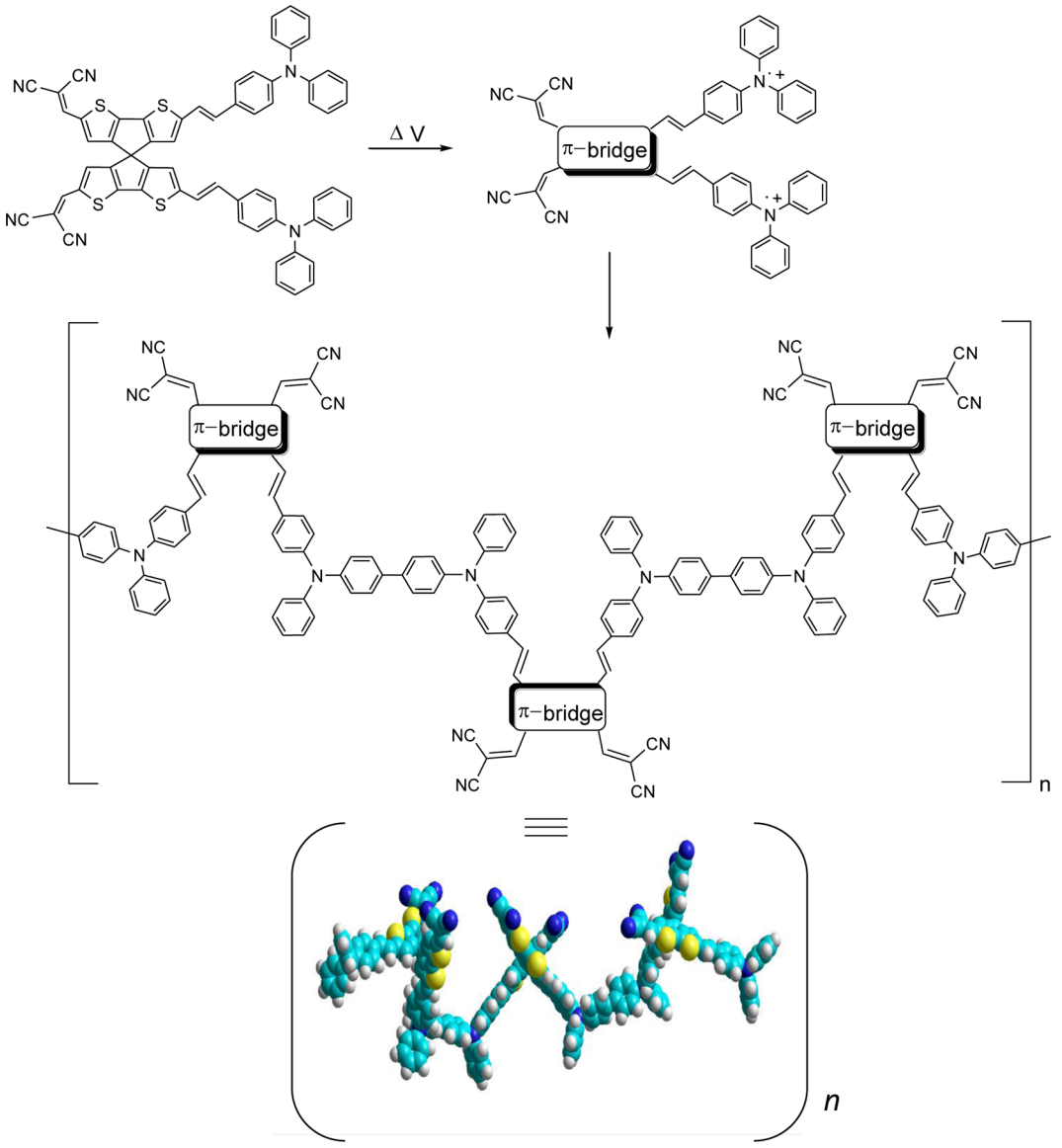

seen that the trace at 450 nm reaches a maximum and decreases as the potential become more anodic. On the other hand, it is clearly seen that the trace at 750 nm reaches a maximum when the film is fully oxidized. During the reverse scan the traces present a similar behavior until these reach the original values, indicating the stability of the material, and the reversibility of the redox processes.

The experimental electrochemical and spectroelectrochemical data here reported are in fully concordance with the presence of TPB in the polymeric film.[10,17,49] Applying anodic potential to the electrode in a solution of **SO1** (Figure 4b) produces TPA radical cations which react forming TPB units and an electroactive film at the electrode surface (see Scheme 2).

Therefore, upon oxidation of the generated film (Figure 5), the absorption due to the generation of TPB radical cation and dication can be observed (Figure 7). At the first oxidation stages TPB radical cations are formed, whose light absorption at around 450 nm is masked by the absorption decreasing of the ITC transition. However, the radical cation formation is clearly documented by the 450 nm trace of Figure 7c. In the forward scan, the absorption intensity at this wavelength first grows and then decreases due to dication appearance (750 nm trace), and it reappears after dication reduction in backward scan.[10,17,49] On the other hand, it should be noted that the broad band centered at around 750 nm is already present when the film is under cathodic applied bias, indicating that a doping degree remains in the film after its formation under the above-mentioned experimental conditions. Such an occurrence is typical in this kind of electroactive polymer films, and it has been previously described by us and other authors for a similar electropolymerization methodology.[10,22,50]

On the other hand, the closely related compound **SO2** was not able to form films through electropolymerization. Therefore, in order to investigate the intermediate species formed by **SO2** in the redox process, the spectroelectrochemical experiments were carried out in a thin layer cell formed by two ITO electrodes. This allowed to record absorption spectra of the species in solution during a CV cycle (see Experimental Section). Figure 8 shows absorption spectra of **SO2** in solution at different applied potentials, which are plotted as Abs and ΔAbs vs wavelength. It can be seen that between −0.2 and 0.5

DOI: 10.1021/acs.macromol.5b00845
Macromolecules XXXX, XXX, XXX−XXX

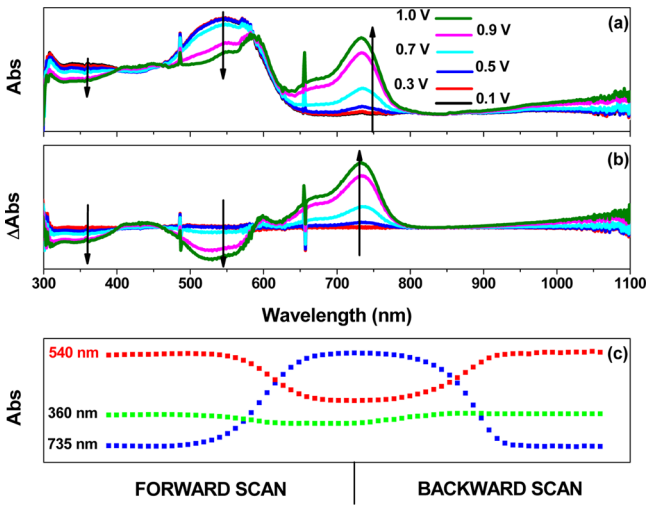

Figure 8. (a) Absorption spectra of **SO2** in DCE with 0.1 M of TBAP, recorded in an ITO thin layer cell at various applied potentials. (b) Spectra plotted ΔAbs. (c) Absorption traces at selected wavelengths as a function of the advances in the forward and backward CV scans.

V there are almost no changes in the absorption spectra, but at around 0.7 V (beginning of the second oxidation potential) a new sharp band at 735 nm with a shoulder at 670 nm starts to appear. At more anodic potentials this band becomes more intense and defined. At the same time, bleaching of the charge transfer band (centered around 540 nm), together with a similar effect in the $\pi-\pi^*$ electronic transition wavelength region, occurs. This behavior is also evidenced in the absorption traces plot (Figure 8c).

Indeed, during the oxidation scan the Abs at 735 nm increases with the concomitant decrease of the trace at 540 nm. Both traces switch then back to their irrespective initial values at the end of the reduction scan. These variations are in agreement with the obtained electrochemical data. As discussed above, **SO2** presents two oxidation peaks: the first one corresponding to the oxidation of the cyclopentadithiophene bridge and the second one to the oxidation of the TPA unit giving rise to a stable radical cation. Similar TPA radical cations, which presented absorption spectra with a sharp band and a shoulder at comparable wavelengths, had been previously observed.[48,49]

The present findings show that upon oxidation **SO2** generates TPA radical cations, which do not undergo dimerization process to form TPB under the experimental condition employed. The lack of dimerization prevents the formation of an electroactive film. In order to get more insight about the different electrochemical behavior of **SO#** dyes, we performed calculations on singly occupied molecular orbitals (SOMO) under the unrestricted Hartree−Fock (UHF) formalism. The calculated spin densities in TPA para positions of the oxidized species for both monomers are similar. Thus, we cannot attribute the difference between **SO#** monomers in the TPA coupling to different spin densities in the reactive positions. Therefore, the low reactivity of **SO2** oxidized species observed in the electrochemical and spectroelectrochemical experiments could be due to entropic effects. In fact, the presence of the vinyl residue connecting the cyclopentadithiophene core and the TPA residue in **SO1** confers to this monomer a higher rotational freedom degree than **SO2**. As consequence, when a potential cycling is applied to a **SO1** solution in the anodic direction, a polymeric material holding electron donor−acceptor centers is formed by electropolymerization. This material has the capacity to generate photoinduced charge separated states, with light absorption in a broad region of the visible spectrum thanks to the particular structural characteristic of the **SO1** molecule.

CONCLUSIONS

Based on the selective functionalization of the symmetrical spiro-configured cyclopentadithiophene core, the synthesis of electron donor−acceptor dyes with broad electronic absorption spectra in the visible region has been achieved. Electrochemical studies have shown that the choice of TPA as the electron donor unit, in combination with the spiro configuration which inhibits the π-conjugation between two D−A branches, is compatible with the formation of a photoelectroactive polymer that retains the original photoinduced donor−acceptor capability. Thus, the polymer film obtained from the electrochemical oxidation of the monomer **SO1**, featuring a vinylene spacer between the TPA unit and the SCPDT core, showed reversible electrochemical processes and stable color changes, in agreement with the TPA dimerization mechanism involved in the electropolymerization process. Upon electrooxidation of the homologue **SO2** molecule, TPA radical cations were also generated, as determined through thin layer spectroelectrochemistry, but in this case the formation of a polymeric film was not observed. The different behavior of **SO1** and **SO2** is likely related to an increased stability of the TPA radicals caused by the direct bonding of the electron donor residues to the SCPDT core. This proposal is strengthened by the electrochemical reversibility observed in **SO2** cyclic voltammetry analysis.

AUTHOR INFORMATION

Corresponding Authors

*E-mail gianluca.pozzi@istm.cnr.it (G.P.).
*E-mail ffungo@exa.unrc.edu.ar (F.F.).

Notes

The authors declare no competing financial interest.

ACKNOWLEDGMENTS

We are grateful to Consejo Nacional de Investigaciones Científicas y Técnicas (CONICET-Argentina), Agencia Nacional de Promoción Científica y Tecnológica (ANPCYT-Argentina), Secretaría de Ciencia y Técnica de la Universidad Nacional de Río Cuarto (SECYT-UNRC), CNR ("Energy from Renewable Sources") and CNR/Regione Lombardia ("Technologies and materials for the efficient use of solar energy") for financial support. M.G., L.O., and F.F are scientific members of CONICET.

REFERENCES

(1) Scharber, M. C.; Sariciftci, N. S. *Prog. Polym. Sci.* **2013**, *38*, 1929−1940.
(2) You, J.; Dou, L.; Yoshimura, K.; Kato, T.; Ohya, K.; Moriarty, T.; Emery, K.; Chen, C.; Gao, J.; Li, G.; Yang, Y. *Nat. Commun.* **2013**, *4* (80), 1446.
(3) Po, R.; Bernardi, A.; Calabrese, A.; Carbonera, C.; Corso, G.; Pellegrino, A. *Energy Environ. Sci.* **2014**, *7*, 925−943.
(4) Dongaonkar, S.; Loser, S.; Sheets, E. J.; Zaunbrecher, K.; Agrawal, R.; Marks, T. J.; Alam, M. A. *Energy Environ. Sci.* **2013**, *6*, 782−787.

DOI: 10.1021/acs.macromol.5b00845
Macromolecules XXXX, XXX, XXX−XXX

(5) Li, M.; Tang, S.; Shen, F.; Liu, M.; Xie, W.; Xia, H.; Liu, L.; Tian, L.; Xie, Z.; Lu, P.; Hanif, M.; Lu, D.; Cheng, G.; Ma, Y. *J. Phys. Chem. B* **2006**, *110*, 17784−17789.
(6) Yang, Y.; Mielczarek, K.; Zakhidov, A.; Hu, W. *ACS Appl. Mater. Interfaces* **2014**, *6*, 19282−19287.
(7) Li, M.; Ishihara, S.; Akada, M.; Liao, M.; Sang, L.; Hill, J. P.; Krishnan, V.; Ma, Y.; Ariga, K. *J. Am. Chem. Soc.* **2011**, *133*, 7348−7351.
(8) Gu, C.; Chen, Y.; Zhang, Z.; Xue, S.; Sun, S.; Zhang, K.; Zhong, C.; Zhang, H.; Pan, Y.; Lv, Y.; Yang, Y.; Li, F.; Zhang, S.; Huang, F.; Ma, Y. *Adv. Mater.* **2013**, *25*, 3443−3448.
(9) Tallman, D. E.; Dewald, M. P.; Vang, C. K.; Wallace, G. G.; Bierwagen, G. P. *Curr. Appl. Phys.* **2004**, *4*, 137−140.
(10) Otero, L.; Sereno, L.; Fungo, F.; Liao, Y.-L.; Lin, C.-Y.; Wong, K.-T. *Chem. Mater.* **2006**, *18*, 3495−3502.
(11) Natera, J.; Otero, L.; D'Eramo, F.; Sereno, L.; Wang, N.-S.; Tsai, Y.-M.; Wong, K.-T.; Fungo, F. *Macromolecules* **2009**, *42*, 626−635.
(12) Fungo, F.; Fernandez, L.; Otero, L.; Liao, Y.-L.; Lin, C.-Y.; Wong, K.-T.; Zabel, P.; Dittrich, T. *Org. Electron.* **2009**, *10*, 1307−1313.
(13) Vacareanu, L.; Grigoras, M. *High Perform. Polym.* **2011**, *23*, 112−124.
(14) Durantini, J.; Otero, L.; Funes, M.; Durantini, E. N.; Fungo, F.; Gervaldo, M. *Electrochim. Acta* **2011**, *56*, 4126−4134.
(15) Durantini, J.; Morales, G. M.; Santo, M.; Funes, M.; Durantini, E. N.; Fungo, F.; Dittrich, T.; Otero, L.; Gervaldo, M. *Org. Electron.* **2012**, *12*, 604−614.
(16) Koyuncu, F. B.; Sefer, E.; Koyuncu, S.; Ozdemir, E. *Macromolecules* **2011**, *44*, 8407−8414.
(17) Mangione, M. I.; Spanevello, R. A.; Rumbero, A.; Heredia, D.; Marzari, G.; Fernandez, L.; Otero, L.; Fungo, F. *Macromolecules* **2013**, *46*, 4754−4763.
(18) Wang, J.; Higashihara, T. *Polym. Chem.* **2013**, *4*, 5518−5526.
(19) Schubert, M.; Dolfen, D.; Frisch, J.; Roland, S.; Steyrleuthner, R.; Stiller, B.; Chen, Z.; Scherf, U.; Koch, N.; Facchetti, A.; Neher, D. *Adv. Energy Mater.* **2012**, *2*, 369−380.
(20) McNeill, C. R.; Abrusci, A.; Hwang, I.; Ruderer, M. A.; Muller-Buschbaum, P.; Greenham, N. C. *Adv. Funct. Mater.* **2009**, *19*, 3103−3111.
(21) Usluer, O.; Koyuncu, S.; Demic, S.; Janssen, R. J. A. *J. Polym. Sci., Part B: Polym. Phys.* **2011**, *49*, 333−341.
(22) Heredia, D.; Fernandez, L.; Otero, L.; Ichikawa, M.; Lin, C.-Y.; Liao, Y.-L.; Wang, S.-A.; Wong, K.-T.; Fungo, F. *J. Phys. Chem. C* **2011**, *115*, 21907−21914.
(23) Saragi, T. P. I.; Spehr, T.; Siebert, A.; Fuhrmann-Lieker, T.; Salbeck, J. *Chem. Rev.* **2007**, *107*, 1011−1065.
(24) Pudzich, R.; Fuhrmann-Lieker, T.; Salbeck, J. *Adv. Polym. Sci.* **2006**, *199*, 83−142.
(25) Hsu, C.-Y.; Chen, Y.-C.; Lin, R. Y.-Y.; Ho, K.-C.; Lin, J. T. *Phys. Chem. Chem. Phys.* **2012**, *14*, 14099−14109.
(26) Grisanti, L.; Terenziani, F.; Sissa, C.; Cavazzini, M.; Rizzo, F.; Orlandi, S.; Painelli, A. *J. Phys. Chem. B* **2011**, *115*, 11420−11430.
(27) Polo, F.; Rizzo, F.; Veiga-Gutierrez, M.; De Cola, L.; Quici, S. *J. Am. Chem. Soc.* **2012**, *134*, 15402−15409 and references therein.
(28) Fungo, F.; Wong, K.-T.; Ku, S.-Y.; Hung, Y.-Y.; Bard, A. J. *J. Phys. Chem. B* **2005**, *109*, 3984−3989.
(29) Samuel, I. D. W.; Turnbull, G. A. *Chem. Rev.* **2007**, *107*, 1272−1295.
(30) Natera, J.; Otero, L.; Sereno, L.; Fungo, F.; Wang, N.-S.; Tsai, Y.-M.; Hwu, T.-Y.; Wong, K.-T. *Macromolecules* **2007**, *40*, 4456−4463.
(31) Duan, L.; Hou, L.; Lee, T.-W.; Qiao, J.; Zhang, D.; Dong, G.; Wang, L.; Qiu, Y. *J. Mater. Chem.* **2010**, *20*, 6392−6407 and references therein.
(32) Isenberg, C.; Saragi, T. P. I. *J. Mater. Chem. C* **2014**, *2*, 8569−8577.
(33) Nguyen, W. H.; Bailie, C. D.; Unger, E. L.; McGehee, M. D. *J. Am. Chem. Soc.* **2014**, *136*, 10996−11001.
(34) Dualeh, A.; Moehl, T.; Nazeeruddin, M. K.; Grätzel, M. *ACS Nano* **2013**, *7*, 2292−2301.
(35) Grancini, G.; Kumar, R. S. S.; Maiuri, M.; Fang, J.; Huck, W. T. S.; Alcocer, M. J. P.; Lanzani, G.; Cerullo, G.; Petrozza, A.; Snaith, H. J. *J. Phys. Chem. Lett.* **2013**, *4*, 442−447.
(36) Fantacci, S.; De Angelis, F.; Nazeeruddin, M. K.; Grätzel, M. *J. Phys. Chem. C* **2011**, *115*, 23126−23133.
(37) Pozzi, G.; Orlandi, S.; Cavazzini, M.; Minudri, D.; Macor, L.; Otero, L.; Fungo, F. *Org. Lett.* **2013**, *15*, 4642−4645.
(38) Yen, H.-J.; Liou, G.-S. *Polym. Chem.* **2012**, *3*, 255−264.
(39) Heo, J.; Oh, J.-W.; Ahn, H.-I.; Lee, S.-B.; Cho, S.-E.; Kim, M.-R.; Lee, J.-K.; Kim, N. *Synth. Met.* **2010**, *160*, 2143−2150.
(40) Cardona, C. M.; Li, W.; Kaifer, A. E.; Stockdale, D.; Bazan, G. C. *Adv. Mater.* **2011**, *23*, 2367−2371.
(41) Yang, S. Y.; Kan, Y. H.; Yang, G. C.; Su, Z. M.; Zhao, L. *Chem. Phys. Lett.* **2006**, *429*, 180−184.
(42) Londenberg, J. Synthese und Charakterisierung von Spirocyclopentadithiophenen PhD Dissertation, University of Kassel,2007.
(43) Londenberg, J.; Saragi, T. P. I.; Suske, I.; Salbeck, J. *Adv. Mater.* **2007**, *19*, 4049−4053.
(44) Romero-Nieto, C.; Merino, S.; Rodríguez-López, J.; Baumgartner, T. *Chem.—Eur. J.* **2009**, *15*, 4135−4145 and references therein.
(45) Duan, T.; Fan, K.; Zhong, C.; Chen, X.; Peng, T.; Qin, J. *J. Power Sources* **2013**, *234*, 23−30.
(46) Chai, Q.; Li, W.; Wu, Y.; Pei, K.; Liu, J.; Geng, Z.; Tian, H.; Zhu, W. *ACS Appl. Mater. Interfaces* **2014**, *6*, 14621−14630.
(47) Namuangruk, S.; Fukuda, R.; Ehara, M.; Meeprasert, J.; Khanasa, T.; Morada, S.; Kaewin, T.; Jungsuttiwong, S.; Sudyoadsuk, T.; Promarak, V. D. *J. Phys. Chem. C* **2012**, *116*, 25653−25663.
(48) Barlow, S.; Odom, S. A.; Lancaster, K.; Getmanenko, Y.; Mason, R.; Coropceanu, V.; Bredas, J.-L.; Marder, S. R. *J. Phys. Chem. B* **2010**, *114*, 14397−14407.
(49) Yurchenko, O.; Freytag, D.; Borg, L.; Zentel, R.; Heinze, J.; Ludwigs, S. *J. Phys. Chem. B* **2012**, *116*, 30−39.
(50) Li, M.; Tang, S.; Shen, F.; Liu, M.; Li, F.; Lu, P.; Lu, D.; Hanif, M.; Ma, Y. *J. Electrochem. Soc.* **2008**, *155*, H287−H291.

DOI: 10.1021/acs.macromol.5b00845
Macromolecules XXXX, XXX, XXX−XXX